



HAL
open science

The USH2A c.2299delG mutation: dating its common origin in a Southern European population.

José M Millán, Elena Aller, Lise Larrieu, Teresa Jaijo, David Baux, Carmen Espinós, Fernando González-Candelas, Carmen Najera, Francesc Palau, Mireille Claustres, et al.

► To cite this version:

José M Millán, Elena Aller, Lise Larrieu, Teresa Jaijo, David Baux, et al.. The USH2A c.2299delG mutation: dating its common origin in a Southern European population.. *European Journal of Human Genetics*, 2010, n/a (n/a), pp.n/a-n/a. 10.1038/ejhg.2010.14 . hal-00509048

HAL Id: hal-00509048

<https://hal.science/hal-00509048>

Submitted on 10 Aug 2010

HAL is a multi-disciplinary open access archive for the deposit and dissemination of scientific research documents, whether they are published or not. The documents may come from teaching and research institutions in France or abroad, or from public or private research centers.

L'archive ouverte pluridisciplinaire **HAL**, est destinée au dépôt et à la diffusion de documents scientifiques de niveau recherche, publiés ou non, émanant des établissements d'enseignement et de recherche français ou étrangers, des laboratoires publics ou privés.

TITLE:

The *USH2A* c.2299delG mutation: dating its common origin in a Southern European population.

RUNNING TITTLE: Allelic age of the *USH2A* c.2299delG mutation.

AUTHORS:

Elena Aller^{1,2}, Lise Larrieu³, Teresa Jaijo^{1,2}, David Baux³, Carmen Espinós², Fernando González-Candelas⁴, Carmen Nájera⁵, Francesc Palau^{2,6}, Mireille Claustres^{3,7,8}, Anne-Françoise Roux^{3,7}, José M Millán^{1,2}.

AFFILIATIONS:

¹Unidad de Genética, Hospital Universitario La Fe, Valencia, Spain.

²CIBER de Enfermedades Raras (CIBERER), Valencia, Spain.

³CHU Montpellier, Laboratoire de Génétique Moléculaire, Montpellier, France.

⁴Instituto Cavanilles de Biodiversidad y Biología Evolutiva, Universitat de València: Genómica y Salud (CSISP, Valencia) and CIBERESP, Spain.

⁵Departamento de Genética, Universitat de València, Valencia, Spain

⁶Unidad de Genética y Medicina Molecular, Instituto de Biomedicina de Valencia (CSIC), Valencia, Spain.

⁷Inserm, U827, Montpellier, France.

⁸Univ, Montpellier I, Montpellier, France.

Corresponding author:

Jose M Millán, PhD

Unit of Genetics

Hospital Universitario La Fe

Avda. Campanar, 21

46009 Valencia. Spain

Tel. +34 96 197 3153

Email. millan_jos@gva.es

chema_millan@yahoo.es

ABSTRACT

Usher syndrome type II is the most common form of Usher syndrome. *USH2A* is the main responsible gene of the three known to be disease causing. It encodes two isoforms of the protein usherin. This protein is part of an interactome that plays an essential role in the development and function of inner ear hair cells and photoreceptors. The gene contains 72 exons spanning over a region of 800 kb. Although numerous mutations have been described, the c.2299delG mutation is the most prevalent in several populations. Its ancestral origin was previously suggested after the identification of a common core haplotype restricted to 250 kb in the 5' region, which encodes the short usherin isoform. By extending the haplotype analysis over the 800 kb region of the *USH2A* gene with a total of 14 intragenic SNPs, we have been able to define 10 different c.2299delG haplotypes showing high variability but preserving the previously described core haplotype. An exhaustive c.2299delG/control haplotype study suggests that the major source of variability in the *USH2A* gene is recombination. Furthermore, we have evidenced twice the amount of recombination hotspots located in the 500 kb that covers the 3' end of the gene, explaining the higher variability observed in this region when compared to the 250 kb of the 5' region. Our data confirm the common ancestral origin of the c.2299delG mutation.

KEYWORDS:

***USH2A*, c.2299delG, haplotype, dating**

INTRODUCTION

Usher syndrome type II (USH2) belongs to a genetically and phenotypically heterogeneous group of recessively inherited disorders that combine hearing loss and retinitis pigmentosa (RP). More specifically, USH2 displays moderate to severe hearing loss, postpubertal onset of RP and normal vestibular reflexes. Although three genes are responsible for USH2, *USH2A* accounts for more than 75% of USH2 cases^{1, 2}. Usher syndrome type IIA (USH2A; MIM 276901) represents the most common form of inherited deaf-blindness and is estimated to affect 1 in 17 000 individuals³.

The underlying *USH2A* gene was isolated by positional cloning⁴. It was initially described as including 21 exons, with the first exon being entirely non-coding, spanning a region of 250 kb and it was predicted to encode a 1 546 amino acid protein of 171 KDa. Today, this protein is recognized as the short isoform of usherin and is predicted to be a secreted extracellular protein^{4, 5}.

Because mutation detection rates obtained in mutation screening studies were lower than those expected, the existence of additional uncharacterised exons of *USH2A* was postulated. van Wijk *et al.*⁶ identified 51 novel exons at the 3' end of the gene increasing its size to 800 kb. These authors also provided some indications for alternative splicing. The predicted protein encoded by the longest open reading frame (5 202 residues) is a member of the protein network known as the Usher interactome. This interactome plays an essential role in the development of the stereocilia of the hair cells in the organ of Corti. In photoreceptors, the Usher interactome localises in the periciliary region and could be involved in the cargo transport between the inner and outer segment^{7- 9}.

Since the identification of the *USH2A* long isoform, a small number of mutation screenings have been reported, which indicates that the study of all 72 exons is mandatory for efficient

molecular diagnosis^{1, 2, 10-13}. As a result of these studies, together with the mutations of the short isoform reported before 2004, more than 210 mutations have been described. A great majority of these mutations are private or present in a few families¹⁴. However, a prevalent mutation located in exon 13, designated as c.2299delG, is frequently found in European and US patients but also in isolated cases from South America, South Africa and Asia. The allele frequency distribution of c.2299delG varies geographically in Europe. This mutation accounts for 47.5% of *USH2A* alleles in Denmark and for 36% in Scandinavia²; while an allelic frequency of 31% was found in the Netherlands¹⁵; 16 to 36 % in the UK^{16, 17}, 15% in Spain¹⁰ and 10% in France (unpublished results). A common ancestral origin has been hypothesised for the c.2299delG mutation on the basis that alleles bearing the c.2299delG mutation share the same core haplotype, restricted to the first 21 exons of the *USH2A* gene¹⁸. In this study, we carry out an exhaustive analysis of the 51 additional exons of the long isoform which reveals high variability in numerous associated intragenic Single Nucleotide Polymorphisms (SNPs) giving rise to, at least, 10 different c.2299delG haplotypes; but preserving the previously described core haplotype. All these data confirm the common origin of this ancestral mutation.

MATERIAL AND METHODS

Patients

Twenty-seven patients were included in this study. Seventeen were of Spanish origin and were recruited from the Federación de Asociaciones de Afectados de Retinosis Pigmentaria del Estado Español (FAARPEE) and from the Ophthalmology and ENT Services of several Spanish hospitals. Ten patients were French and were recruited from medical genetic and ophthalmology clinics distributed all over France. The patients were classified as Usher type

II on the basis of ophthalmologic studies, including visual acuity, visual field and fundus ophthalmoscopy, electroretinography, pure-tone and speech audiometry and vestibular evaluation. For each patient, samples from parents were considered as well as siblings, when possible. This study was approved by both the Hospital La Fe and CHU Montpellier Ethical Committees and consent to genetic testing was obtained from adult probands or parents in the cases of minors.

Controls

97 control chromosomes were used to establish the distribution of *USH2A* normal alleles. They were generated from fifty trios (subject and both parents). Twenty-five of each were of French and Spanish origins and randomly chosen as the healthy control group. These trios did not refer symptoms or a history of Usher syndrome or related disorders.

DNA analysis of *USH2A* gene

Patient and control genomic DNA was extracted from peripheral blood samples using standard protocols. The 14 SNPs used to construct *USH2A* haplotypes of control and c.2299delG alleles were PCR-amplified using the primers and PCR conditions previously described^{5, 6}. PCR products were directly sequenced on an ABI PRISM 3130xl (Applied Biosystems, CA, U.S.A). The polymorphism IVS17-8T>G was not considered in this study. Because this variant was included in the core haplotypes defined by Dreyer *et al.*¹⁸ we indicate it in brackets to avoid any confusion when referring to Dreyer's data.

Construction of haplotypes

Parents and available siblings of the c.2299delG patients were used to infer the haplotypes linked to the c.2299delG mutation (M haplotypes). Similarly, control trios were used to establish normal *USH2A* haplotypes in a healthy population (C haplotypes). In all cases haplotypes were manually generated by inheritance. In some cases, the data were not

informative enough to establish the phase of the SNPs and some ambiguities remained. When possible, ambiguous haplotypes were ascribed to an already existing haplotype.

Construction of phylogenetic trees.

Relationships between haplotypes were inferred using two approaches with three different data sets: the complete set of SNPs, the first five SNPs included in the first 21 exons of the gene, and the last 9 SNPs located in the 3' end of the gene (see table 1). In the first approach, we constructed phylogenetic trees using a variety of methods and evolutionary models. However, the high levels of homoplasy present in this dataset prevented the derivation neither of a single most reliable phylogenetic tree, neither with the whole set nor with any of the other subsets of SNPs. Among the different trees obtained, we present the results obtained with the neighbor-joining method¹⁹, using the uncorrected number of differences between pairs of SNPs as a measure of their genetic divergence. Bootstrap support values were obtained using version 4.1 of the MEGA software.

Additionally, a median-joining network was obtained with the program Network 4.5.10 (Fluxus Technology, <http://www.fluxus-technology.com>). A network represents all the alternative possibilities linking every haplotype considered through a minimum number of mutation steps and is not restricted to represent relationships as a single pathway. This is a more appropriate methodology than dichotomous phylogenetic trees for establishing relationships among closely related allele variants²⁰.

Dating the *USH2A* c.2299delG mutation

To estimate the original date of the c.2299delG mutation in the *USH2A* gene three mathematical approaches were applied: a Monte Carlo likelihood method implemented in the program BDMC21 v2.1²¹ (<http://www.rannala.org/labpages/software.html>), a Markov chain

method by means of the DMLE+ v2.2 software²²⁻²⁴ (<http://www.dmle.org>) and a moment method described by Bengtsson and Thomson²⁵.

The program BDMC21 v2.1 relies on the assumption that genetic variation among a group of highly linked polymorphic markers, defining a haplotype in which a novel non-recurrent mutation arose, is a function of the mutation frequencies of those linked markers and the time since the first occurrence of this unique mutation. To achieve this approach, we considered information from the three variable SNPs closest to the c.2299delG mutation: c.4714C>T, c.6506T>C and c.6875G>A. Confidence interval was estimated following the standard theory of maximum likelihood estimation²⁶. The second analysis performed was using the DMLE+ program version 2.2, which takes into account the marker information from the entire haplotype on the basis of:

5'_c.373G>A_c.504A>G_c.1419C>T_IVS15+35G>A_c.4457G>A_c.4714C>T_c.6506T>C_c.6875G>A_c.10232A>C_c.11602A>G_c.11677C>A_c.12612A>G_c.12666A>G_c.13191G>A_3'.

This program allows Bayesian inference of the mutation age based on the observed linkage disequilibrium at multiple genetic markers. For both approaches, we used a carrier frequency of USH2 of 1/106, a proportion of mutation-bearing chromosomes in our sample $f=1.7 \times 10^{-5}$, and a population growth parameter $d=0.05$. Moreover, because the estimate of mutation age based on the DMLE+ v2.2 software seems to be sensitive to demographic parameters (growth rate, mutation frequency, and population size)²⁴, we analyzed haplotype data considering a range of plausible growth rates ($d=0.03-0.11$) and proportion of chromosomes ($f=1 \times 10^{-6}-6 \times 10^{-5}$). After this, in order to verify the estimated allele age, we decided to use a method described by Bengtsson and Thomson²⁵ based on the algorithm: $g = \log \delta / \log(1-\theta)$, that depends on the linkage disequilibrium (δ) and on the recombination frequency (θ), and therefore

insensitive to demographic parameters. For this analysis, we considered information from the 3 SNPs showing significant LD index values (δ): c.4714C>T, c.6506T>C and c.10232A>C. SNPs c.373G>A, c.504A>G, c.1419C>T, IVS15+35G>A and c.4457G>A were not informative for this analysis because all disease chromosomes carried the same allele. SNPs c.6875G>A, c.11677C>A and c.12666A>G could not be used in this method because the proportion of disease chromosomes carrying the major allele (Pd) was lower than the proportion of normal chromosomes carrying that same allele (Pn). Finally, to set the genetic clock, we applied the Luria-Delbrück correction: $g_c = g + g_0^{27}$ in order to avoid a possible underestimation²⁸⁻³⁰.

RESULTS

c.2299delG haplotypes

The c.2299delG haplotypes were built for the 27 *USH2A* patients using the 14 SNPs represented in table 1. Seven of the patients were c.2299delG homozygotes (six were Spanish and one was French). A total of 10 different haplotypes were identified (M1-M10, see table 2). The haplotypes were identical from exon 2 to 21, but the SNPs located along the 51 additional exons of the *USH2A* long isoform were variable (Table 2). The variability rate of the SNPs was uneven. For five of the SNPs (c.4714C>T, c.6875G>A, c.11602A>G, c.11677C>A and c.13191G>A) the same allele was present on at least 8 haplotypes.

Haplotype M1 was the most frequent in the Spanish population (8/23; frequency 0.35) followed by haplotype M2 (6/23; frequency of 0.26). Haplotype M1 was also the most prevalent in France, together with haplotype M8 (3/11; frequency 0.27). Haplotypes M4-M9 were restricted to either the Spanish or French populations. Haplotype M1 was the most common with a frequency of 0.32 (11/34) when both populations were pooled.

Control *USH2A* haplotypes

Fifty-four different haplotypes could be defined from the 97 control chromosomes (Supplementary Table 1). Variation was found along the entire gene, however, this variation is significantly higher in the region encompassing from exon 22 to exon 72. Two SNPs remained invariable: c.4714C>T and c.11677C>A. In addition, the c.6875G>A SNP had the same G allele in 53 of 54 haplotypes. Interestingly, this variant corresponds to the only CpG dinucleotide identified among the 14 SNPs (Table 1). Haplotype C1 was the most prevalent among the Spanish control population with a frequency of 0.1 (5/51) and haplotype C6 was the most frequent among the French controls with a frequency of 0.09 (4/46). Combining the data from both populations, haplotype C1 was the most prevalent with a frequency of 0.07 (7/97).

Relationship of haplotypes

The neighbor-joining tree for all the entire haplotypes was rooted with the corresponding *Pan troglodytes* haplotype. It did not present a well-defined structure, since none of the nodes were supported by bootstrap analysis. Nevertheless, a small cluster encompassing six haplotypes related to the disease (M1, M2, M5-M8) was observed. The remaining disease-associated haplotypes did not group with this clade, but were not too distant from it (Supplementary Fig. 1A). This pattern was very different from that obtained when only the 5 SNPs from the first 21 exons of the gene were analyzed. The common haplotype including disease-related alleles as well as many others from control chromosomes occupies an intermediate position between the oldest haplotypes, as inferred from their close relationship to the out-group, and the most recently derived, the group including C40-C46. Again, none of the nodes in this tree were supported by bootstrap analysis (Supplementary Fig. 1B). This topology is markedly different from the one inferred from the remaining SNPs, those located

at the 3'-end of the gene. Here, there was no longer a clear association between disease-related haplotypes, except for a small group including alleles M5-M8. Most of the other disease-related haplotypes were more closely related to control alleles than to any other disease allele but, again, these associations were not supported by bootstrap analysis (Supplementary Fig. 1C).

The apparent lack of congruence between the phylogenetic histories of these alleles when considering SNPs from the 5'- and 3'-ends may be due to frequent recombination events. This was further checked by reconstruction of median-joining networks for the same three data sets described above. The three networks, but especially those derived from the complete and the 3'-end sets of SNPs, present a high level of connectedness with many alternative routes connecting every possible pair of haplotypes (see Supplementary Fig. 2A, 2B and 2C). There are also many haplotypes connected to several others with a minimum number of intermediate steps and only a few haplotypes are connected to the rest through a single intermediate. This pattern is still present, although at a much reduced level, in the network derived from SNPs in the 5'-end of the gene (Supplementary Fig. 2B), partly due to the reduced number of different haplotypes in this part of the gene. The ancestral (C19, which includes *Pan troglodytes*) and the most abundant haplotypes are connected through an intermediate haplotype (either C28 or C17) and two point changes in SNPs c.3157+15G>A and c.4457G>A. These observations easily explain the difficulties encountered in reconstructing a phylogenetic tree with well supported relationships as previously commented. Although it is certainly possible to invoke homoplastic point mutations to explain these patterns, they are more likely due to high level of recombination, with an apparently higher rate in the second part of the gene.

Dating the c.2299delG mutation

We estimated the allele age of the *USH2A* c.2299delG mutation using three mathematical approaches. Haplotype data were analysed for the Spanish and French populations separately and also together in the pooled populations using both the BDMC21 v2.1 program and the DMLE+ v2.2 software. Results were quite similar for both mathematical methods (Table 3). Taken into account the whole studied population, the estimated age of the c.2299delG mutation resulted to be 245.4 generations (95% CI 245.2-245.6) and 231.3 generations (95% CI 204.8-245.6) for the BDMC21 v2.1 program and the DMLE+ v2.2 software, respectively. Assuming a generation time of 28 years³¹, these results indicate that the c.2299delG arose between 6 476-6 871 years ago.

For the DMLE+ v2.2 approach, we found a high variability as a result of the oscillation of the growth rate values between $d= 0.03$ [$g= 374.96$ (95% CI 321.84-464.08)] and $d= 0.11$ [$g= 111.84$ (95% CI 97.39-138.38)] that led to an estimated allelic age of 10 500 years for the former and 3 100 for the latter. The analyzed range of f gave an oscillation of: $g= 288.4$ (95% CI 256.4-346.8) for $f= 1 \times 10^{-6}$, and $g= 204.3$ (95% CI 176.2-260.9) for $f= 6 \times 10^{-5}$, thus ranging from 8 000 to 5 700 years old respectively (Fig. 1A and 1B).

Finally, we analysed LD data using the algorithm $g= \log \delta / \log(1-\theta)$ and the Luria-Delbrück correction. These results showed that the c.2299delG mutation arose 95-206 generations ago and increased to 163-264 generations ago when applying the Luria-Delbrück correction. Assuming a generation time of 28 years³¹, this would indicate that the *USH2A* c.2299delG mutation could have arisen 2 700-5 800 years ago or 4 600-7 400 years ago with the correction (Table 4).

DISCUSSION

The data obtained from the entire haplotypes of the control population reveal a highly variable genetic background, since 54 haplotypes could be identified in the Spanish and French populations with no evidence of a prevalent common haplotype (Supplementary Table 1). In 2001, twelve core haplotypes were identified by Dreyer *et al.*¹⁸ in a Scandinavian control population. These were based on partial information since only part of the *USH2A* gene was then recognized. These authors identified a major haplotype “A-G-C-A-(T)-A” with a frequency of 0.60. This core haplotype is also the most frequent one in our control group (C1 to C16), but overall represents less than 50%. The same core haplotype is found in all c.2299delG alleles within the first 21 exons, confirming the existence of high linkage disequilibrium in this 250 kb region.

The C>T distribution of the c.4714 SNP is quite striking. The C allele is present in all control haplotypes, but it is carried by only two disease-associated haplotypes, M9 and M10, that represent less than 15% of the c.2299delG alleles. Linkage disequilibrium between the c.4714T allele and the c.2299delG mutation had already been noted in a French study¹. Dreyer *et al.*² identified this SNP in both the c.2299delG and control Scandinavian alleles. However, we do not know if the majority of the c.2299delG patients in Northern Europe also carry the T allele at this position. Extending the studies to Northern Europe and other populations should help to clarify this point.

The variability observed in the additional portion of the gene covering from exon 22 to 72 (i.e. about 500 kb) is quite puzzling, suggesting a high recombinational activity at the 3' end of the gene and a conservation of the 5' end. We analyzed the mutability rate of *USH2A* SNPs by looking at CpG dinucleotides (Table 1). Only one CpG was found in exon 36 at position 6875 and, therefore, cannot explain the variability observed in the 3' region. The median-

joining networks reconstructed in order to find the relationship between haplotypes showed a high level of connectedness, especially for the second part of the gene. These networks are more easily explained by the existence of high recombination rates than by point mutations. These analysis using formal methods confirm that recombination events represent the predominant source of variability in this gene. Subsequently, we looked for a common sequence motif CCNCCNTNNCCNC associated with recombination hot spots in humans³² along the entire *USH2A* DNA sequence. Twenty motif locations were found, 4 within the first 20 introns and 16 between introns 21-71. Therefore, twice amount of recombination hotspots are located in the most variable region.

Three different mathematical approaches led to a wide range of estimated allelic age for c.2299delG mutation depending on the methods. When we applied BDMC21 and DMLE+, the estimated allelic age ranged from about 5 500 to 7 000 years old. When we used variable f and d to correct the sensitivity of these methods to demographic parameters, the allelic age ranged from 3 100 to 10 500 years old. Finally, using a method based on genetic parameters, we obtained an estimate of 2 700-5 800. Labuda *et al.*²⁹ suggested that the genetic clock lead to an underestimation when it is applied to growing populations and used a correction (based on d and f) to avoid this underestimation. When we applied this correction, we obtained a range of ages from 4 500-7 500.

The programs BDMC21 and DMLE+ are highly dependent on demographic parameters. In fact, when one uses a range of d and f , the estimated allelic age varies considerably, reflecting that these programs hardly consider genetic data. Results are strongly biased due to the c.2299delG allelic frequency estimation was only based on clinical data and current prevalence of the disease. Moreover, the overall demographic growth parameter for Europe could not be equivalent to the local growth rate for Spanish and French populations. Thus,

further studies are still to be done considering the rest of the European populations to estimate a more realistic figure for the original date of c.2299delG.

There are no data concerning the c.2299delG frequency among North-Africans. However, c.2299delG is not a prevalent mutation in the non-Ashkenazi Jewish populations from the South and Near East regions^{11, 33, 34}. This supports the hypothesis of the more recent migration fluxes across the Mediterranean Sea as a cause of the reduced frequency of the c.2299delG mutation within Northern Mediterranean populations. Another interesting point is the presence of c.2299delG in Asian patients. This mutation was found in isolated patients of Chinese origin¹⁵. The recent studies carried out by Dai *et al.*¹² in China and Nakanishi *et al.*¹³ in Japan indicate that c.2299delG is not common among Asian USH2 patients, although the authors only screened six and ten patients respectively. Further studies are needed in order to investigate the frequency of c.2299delG in this and other non-European populations.

In relation to those territories with a history of European colonization, such as America and South Africa, it has already been pointed by Dreyer *et al.*¹⁸ that the recent waves of European migration to the New World and other countries would definitely explain the presence of c.2299delG in these populations.

The exhaustive study of the 3' region of the *USH2A* gene in our cohort of patients has revealed that haplotypes linked to the c.2299delG mutation show high variability, but preserve the previously described core haplotype "A-G-C-A-(T)-A". This common haplotype is restricted to 250 kb in the 5' region of this gene, which corresponds to the USH2A protein short isoform. By extending this study to the control population we have evidenced the existence of linkage disequilibrium restricted to this 250 kb region. The analysis of the

relationship between *USH2A* haplotypes suggests that the major source of variability in this gene is recombination. The higher variability observed in the 3' region could be explained by the accumulation of recombination hotspots observed in specific intronic sequences of this portion of the gene. It is difficult to ascertain if the structural and dynamic differences observed between the 5' and 3' region of the gene could have a functional significance. Our data do not allow us to estimate a realistic allelic age for c.2299delG. Nevertheless, this mutation appears to have a European ancestral origin.

ACKNOWLEDGEMENTS

Authors are grateful to the participating patients and their relatives and to the FAARPEE for their help and co-operation. This work was supported by grants from the Fondo de Investigaciones Sanitarias (FIS07/0558) and from Ministère de la Recherche "PHRC National 2004" (Protocole 7802).

We also acknowledge Fabiola Barraclough for English corrections.

REFERENCES

1. Baux D, Larrieu L, Blanchet C *et al*: Molecular and in silico analyses of the full length isoform of usherin identify new pathogenic alleles in Usher type II patients. *Hum Mutat* 2007, **28**(8):781-9.
2. Dreyer B, Brox V, Tranebjaerg L *et al*: Spectrum of *USH2A* mutations in Scandinavian patients with Usher syndrome type II. *Hum Mutat* 2008, **29**(3):451.

3. Kimberling WJ. Estimation of the frequency of occult mutations for an autosomal recessive disease in the presence of genetic heterogeneity: application to genetic hearing loss disorders. *Hum Mutat* 2005, **26**(5):462-70.
4. Eudy JD, Weston MD, Yao S *et al*: Mutation of a gene encoding a protein with extracellular matrix motifs in Usher syndrome type IIa. *Science* 1998, **280**(5370):1753-7.
5. Weston MD, Eudy JD, Fujita S *et al*: Genomic structure and identification of novel mutations in usherin, the gene responsible for Usher syndrome type IIa. *Am J Hum Genet* 2000, **66**(4):1199-210.
6. Van Wijk E, Pennings RJ, te Brinke H *et al*: Identification of 51 novel exons of the Usher syndrome type 2a (USH2A) gene that encode multiple conserved functional domains and that are mutated in patients with Usher syndrome type II. *Am J Hum Genet* 2004, **74**(4):738-44.
7. Adato A, Lefèvre G, Delprat B *et al*: Usherin, the defective protein in Usher syndrome type IIA, is likely to be a component of interstereocilia ankle links in the inner ear sensory cells. *Hum Mol Genet* 2005, **14**(24):3921-32.
8. Liu X, Bulgakov OV, Darrow KN *et al*: Usherin is required for maintenance of retinal photoreceptors and normal development of cochlear hair cells. *Proc Natl Acad Sci U S A*. 2007, **104**(11):4413-8.
9. Maerker T, van Wijk E, Overlack N *et al*: A novel Usher protein network at the periciliary reloading point between molecular transport machineries in vertebrate photoreceptor cells. *Hum Mol Genet* 2008, **17**(1):71-86.

10. Aller E, Jaijo T, Beneyto M *et al*: Identification of 14 novel mutations in the long isoform of USH2A in Spanish patients with Usher syndrome type II. *J Med Genet* 2006, **43**(11):e55.
11. Auslender N, Bandah D, Rizel L *et al*: Four USH2A Founder Mutations Underlie the Majority of Usher Syndrome Type 2 Cases among Non-Ashkenazi Jews. *Genet Test* 2008, **(2)**:289-94.
12. Dai H, Zhang X, Zhao X *et al*: Identification of five novel mutations in the long isoform of the USH2A gene in Chinese families with Usher syndrome type II. *Mol Vis* 2008, **14**:2067-75.
13. Nakanishi H, Ohtsubo M, Iwasaki S, Hotta Y, Mizuta K, Mineta H, Minoshima S. Identification of 11 novel mutations in USH2A among Japanese patients with Usher syndrome type 2. *Clin Genet* 2009, **8**. [Epub ahead of print].
14. Baux D, Faugère V, Larrieu L *et al*: UMD-USHbases: a comprehensive set of databases to record and analyse pathogenic mutations and unclassified variants in seven Usher syndrome causing genes. *Hum Mutat* 2008, **29**(8):E76-E87.
15. Pennings RJ, Te Brinke H, Weston MD *et al*: USH2A mutation analysis in 70 Dutch families with Usher syndrome type II. *Hum Mutat* 2004, **24**(2):185.
16. Liu XZ, Hope C, Liang CY *et al*: A mutation (2314delG) in the Usher syndrome type IIA gene: high prevalence and phenotypic variation. *Am J Hum Genet* 1999, **64**(4):1221-5.
17. Leroy BP, Aragon-Martin JA, Weston MD *et al*: Spectrum of mutations in USH2A in British patients with Usher syndrome type II. *Exp Eye Res* 2001, **72**(5):503-9.
18. Dreyer B, Tranebjaerg L, Brox V *et al*: A common ancestral origin of the frequent and widespread 2299delG USH2A mutation. *Am J Hum Genet* 2001, **69**(1):228-34.

19. Saitou N and Nei M: The neighbor-joining method: a new method for reconstructing phylogenetic trees. *Mol Biol Evol* 1987, **4**:406-25.
20. Bandelt H-J, Forster P, Röhl A: Median-joining networks for inferring intraspecific phylogenies. *Mol Biol Evol* 1999, **16**:37-48).
21. Slatkin, M. and Rannala, B: Estimating the age of alleles by use of intraallelic variability. *Am J Hum Genet* 1997, **60**, 447-58.
22. Rannala, B. and Slatkin, M: Likelihood analysis of disequilibrium mapping, and related problems. *Am J Hum Genet* 1998, **62**, 459-73.
23. Reeve, J.P. and Rannala, B. DMLE+: Bayesian linkage disequilibrium gene mapping. *Bioinformatics* 2002, **18**, 894-5.
24. Rannala, B. and Reeve, J.P: Joint Bayesian estimation of mutation location and age using linkage disequilibrium. *Pac Symp Biocomput* 2003, 526-34.
25. Bengtsson, BO and Thomson, G: Measuring the strength of associations between HLA antigens and diseases. *Tissue Antigens* 1981, **18**, 356-63.
26. Sorensen, D.A. and Gianola, D: Likelihood, Bayesian and MCMC methods in quantitative genetics. Springer-Verlag, New York. 2002.
27. Luria SE, Delbrück M. Mutations of bacteria from virus sensitivity to virus resistance. *Genetics* 1943, **28**: 491-511
28. Labuda M, Labuda D, Korab-Laskowska M, Cole DE, Zietkiewicz E, Weissenbach J, Popowska E, Pronicka E, Root AW, Glorieux FH. Linkage disequilibrium analysis in young populations: pseudo-vitamin D-deficiency rickets and the founder effect in French Canadians. *Am J Hum Genet* 1996, **59**(3): 633-43.

29. Labuda D, Zietkiewicz E, Labuda M. The genetic clock and the age of the founder effect in growing populations: a lesson from French Canadians and Ashkenazim. *Am J Hum Genet* 1997, **61**(3): 768-71.
30. Colombo R. Age estimate of the N370S mutation causing Gaucher disease in Ashkenazi Jews and European populations: A reappraisal of haplotype data. *Am J Hum Genet* 2000, **66**(2): 692-7.
31. Fenner JN. Cross-cultural estimation of the human generation interval for use in genetics-based population divergence studies. *Am J Phys Anthropol* 2005, **128**(2): 415-23.
32. Myers S, Freeman C, Auton A, Donnelly P, McVean G: A common sequence motif associated with recombination hot spots and genome instability in humans. *Nat Genet* 2008, **40**:1124-9
33. Adato A, Weston MD, Berry A, Kimberling WJ, Bonne-Tamir A: Three novel mutations and twelve polymorphisms identified in the USH2A gene in Israeli USH2 families. *Hum Mutat* 2000, **15**(4):388.
34. Kaiserman N, Obolensky A, Banin E, Sharon D: Novel USH2A mutations in Israeli patients with retinitis pigmentosa and Usher syndrome type 2. *Arch Ophthalmol* 2007, **125**(2):219-24.

TITLES AND LEGENDS TO FIGURES

Supplementary Figure 1. Phylogenetic trees constructed using *USH2A* haplotypes data.

- A. Neighbor-joining tree constructed using the complete set of SNPs (Hamming distance).

- B. Neighbor-joining tree constructed using the first 5 SNPs (Hamming distance).
- C. Neighbor-joining tree constructed using the last 9 SNPs (Hamming distance).

Pan: *Pan troglodytes*

Supplementary Figure 2. Median-joining networks representing all the alternative possibilities linking every *USH2A* haplotype.

- A. Median-joining network constructed using the complete set of SNPs (Hamming distance).

mv1-mv12 nodes represent haplotypes that have not been found in the sample of study. These haplotypes are automatically generated by programme Network 4.5.10 in order to connect the haplotypes found in our study.

PAN: *Pan troglodytes*.

- B. Median-joining network constructed using the first 5 SNPs (Hamming distance).

M1 node includes haplotypes M1-M10 + C1-C15.

C19 node includes haplotypes C19-C21 + C24-C26 + Pan (*Pan troglodytes*).

C29 node includes haplotypes C29-C31.

C33 node includes haplotypes C33-C35.

C40 node includes haplotypes C40-C46.

C48 node includes haplotypes C48-C49.

C50 node includes haplotypes C50-C51.

C52 node includes haplotypes C52-C53.

C. Median-joining network constructed using the last 9 SNPs (Hamming distance).

mv1-mv12 nodes represent haplotypes that have not been found in the sample of study. These haplotypes are automatically generated by program Network 4.5.10 in order to connect the haplotypes found.

PAN: *Pan troglodytes*.

M9 node includes haplotypes M9, C29 and C47.

M10 node includes haplotypes M10, C14 and C37.

C1 node includes haplotypes C1, C34, C40 and C48.

C2 node includes haplotypes C2 and C25.

C3 node includes haplotypes C3 and C49.

C5 node includes haplotypes C5, C17, C33, C36, C48 and C41.

C6 node includes haplotypes C6, C26, C42 and C53.

C7 node includes haplotypes C7 and C39.

C9 node includes haplotypes C9, C28, C35, C43 and C51.

C15 node includes haplotypes C15, C20, C31 and C46.

C19 node includes haplotypes C19 and C45.

C24 node includes haplotypes C24 and C54.

Figure 1. Estimate of c.2299delG allelic age using DMLE+.

A. Calculated using a variable proportion of mutated chromosomes (*f*)

B. Calculated using a variable population growth rate (*d*)

Table 1. Location and repartition of the 14 SNPs used to establish the *USH2A* haplotypes.

The encoded short and long transcripts are indicated. Total distance between c.373G>A and c.13191G>A is approximately 730 kb. The distance between two SNP can be less than 1 kb. Entrez accession number is indicated for each SNP except for c.4714C>T, which is in linkage disequilibrium with the c.2299delG mutation and is not referenced in dbSNP.

Table 2. Representation of the ten different c.2299delG linked haplotypes.

Supplementary Table 1. Representation of the fifty-four different control *USH2A* haplotypes.

Table 3. Summarized results of c.2299delG dating using BDMC21 and DMLE+ programs.

Results are given in number of generations with a confidence interval of 95%.

Considered data:

Population size: 64×10^6 (France), 42×10^6 (Spain), 106×10^6 (Total).

Number of disease chromosomes: 11 (France), 23 (Spain), 34 (Total).

Proportion of mutation-bearing chromosomes in our sample [f]: 9.109×10^{-6} (France), 2.9024×10^{-5} (Spain), 1.7×10^{-5} (Total).

Table 4. LD Analysis and Corrected Estimated Age (g_c) of the c.2299delG (*USH2A*) mutation in South European patients.

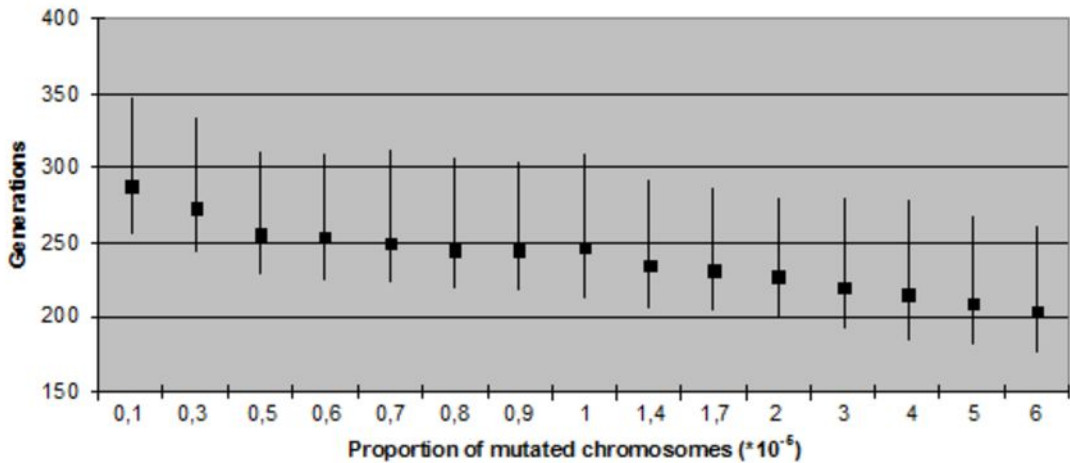
(1) Assuming 900 kb/1 cM

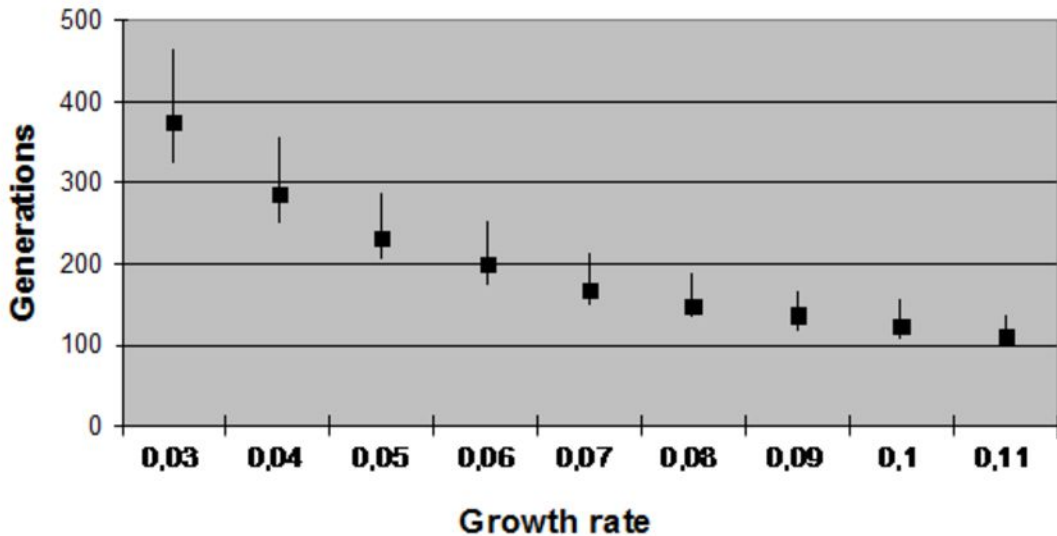
$$(2) g = \log \delta / \log(1 - \theta)$$

$$(3) g_o = -(1/d) \ln(\theta f d), \text{ [assuming } d \text{ (growth parameter)} = 0.05 \text{ and } f d = 1/d]$$

$$(4) g_c = g + g_o$$

(5) Calculated with the assumption of 28 years/generation (Fenner 2005)





SNP (nucleotide nomenclature)	Entrez SNP accession number	Exon	Distances (kb) from the previous SNP	CpG
c.373G>A	rs10779261	2		No
c.504A>G	rs4253963	3	3,3	No
c.1419C>T	rs1805050	8	95	No
c.3157+15G>A	rs1324330	15	106	No
c.4457G>A	rs1805049	21	27	No
c.4714C>T		22	78	No
c.6506T>C	rs10864219	34	98	No
c.6875G>A	rs41277210	36	28	Yes
c.10232A>C	rs10864198	52	184	No
c.11602A>G	rs35309576	60	45	No
c.11677C>A	rs41303285	60	0,07	No
c.12612A>G	rs2797235	63	67	No
c.12666A>G	rs2797234	63	0,05	No
c.13191G>A	rs2009923	63	0,5	No

Table 1. Location and repartition of the 14 SNPs used to establish the *USH2A* haplotypes.

The encoded short and long transcripts are indicated. Total distance between c.373G>A and c.13191G>A is approximately 730 kb. The distance between two SNP can be less than 1 kb. Entrez accession number is indicated for each SNP except for c.4714C>T, which is in linkage disequilibrium with the c.2299delG mutation and is not referenced in dbSNP.

	EXON 2	EXON 3	EXON 8	IVS 15	EXON 21	EXON 22	EXON 34	EXON 36	EXON 52	EXON 60	EXON 60	EXON 63A	EXON 63A	EXON 63B			
	p.A125T	p.T168T	p.T473T	IVS15	p.R1486K	p.L1572F	p.I2169T	p.R2292H	p.E3411A	p.M3868V	p.P3893T	p.T4204T	p.T4222T	p.E4397E	Spain	France	TOTAL
	c.373G>A	c.504A>G	c.1419C>T	+35G>A	c.4457G>A	c.4714C>T	c.6506T>C	c.6875G>A	c.10232A>C	c.11602A>G	c.11677C>A	c.12612A>G	c.12666A>G	c.13191G>A			
M1	A	G	C	A	A	T	T	G	A	A	C	G	A	G	8	3	11
M2	A	G	C	A	A	T	T	G	A	A	C	G	G	G	6	2	8
M3	A	G	C	A	A	T	T	G	A	A	C	A	A	A	2	1	3
M4	A	G	C	A	A	T	T	G	A	A	C	A	A	G	0	1	1
M5	A	G	C	A	A	T	T	G	C	A	C	G	G	G	1	0	1
M6	A	G	C	A	A	T	T	G	C	A	C	G	A	G	1	0	1
M7	A	G	C	A	A	T	C	G	C	A	C	G	A	G	1	0	1
M8	A	G	C	A	A	T	C	A	C	A	A	G	G	G	0	3	3
M9	A	G	C	A	A	C	T	G	C	G	C	G	G	G	2	0	2
M10	A	G	C	A	A	C	C	G	C	G	C	G	A	G	2	1	3
															TOTAL=		34

Table 2. Representation of the ten different c.2299delG linked haplotypes.

	BDMC21 Number of Generations (CI 95%)	DMLE+ Number of Generations (CI 95%)
Spain	226.3 (225.93-226.67)	219.33 (185.44-279.46)
France	234.9 (233.34-236.46)	222.03 (191.19-290.05)
Total	245.4 (245.23-245.57)	231.29 (204.76-245.57)

Table 3. Summarized results of c.2299delG dating using BMC21 and DMLE+ programs.

Results are given in number of generations with a confidence interval of 95%.

Considered data:

Population size: 64×10^6 (France), 42×10^6 (Spain), 106×10^6 (Total).

Number of disease chromosomes: 11 (France), 23 (Spain), 34 (Total).

Proportion of mutation-bearing chromosomes in our sample [f]: 9.109×10^{-6} (France), 2.9024×10^{-5} (Spain), 1.7×10^{-5} (Total).

MARKER	ALLELE	LD ANALYSIS				x^2	P value	δ (Pd-Pn)/(1-Pn)	DISTANCE $\theta(1)$	GENERATIONS			YEARS (5)
		Pd	Pn	g (2)	g ₀ (3)					gc (4)			
c.4714C>T	T	0,853	29/34	0	0/97	106,258	<0,001	0,853	0,00167	95,12750483	67,98398758	163,1114924	4567,121788
c.6506T>C	T	0,794	27/34	0,526	51/97	7,526	<0,01	0,565	0,00276	206,5729356	57,93584651	264,5087821	7406,245898
c.10232A>C	A	0,676	23/34	0,392	38/97	8,202	<0,01	0,467	0,0051	148,9181824	45,65564931	194,5738317	5448,067289
c.11602A>G	A	0,853	29/34	0,722	70/97	2,351	<0,5	NS					
c.12612A>G	G	0,882	30/34	0,866	84/97	0,06	<0,5	NS					
c.13191G>A	G	0,912	31/34	0,887	86/97	0,167	>0,5	NS					

Table 4. LD Analysis and Corrected Estimated Age (gc) of the c.2299delG (*USH2A*) mutation in South European patients.

(1) Assuming 900 kb/1 cM

(2) $g = \log \delta / \log(1 - \theta)$

(3) $g_0 = -(1/d) \ln(\theta f d)$, [assuming d (growth parameter) = 0.05 and $f d = 1/d$]

(4) $gc = g + g_0$

(5) Calculated with the assumption of 28 years/generation (Fenner 2005)